About some relevant aspects regarding WENO type schemes on the shock tube problem

Alina BOGOI[1], Sterian DANAILA*,[1], Dragos ISVORANU[1]

*Corresponding author
[1]Department of Aerospace Engineering, Politehnica University of Bucharest,
Splaiul Independenţei 313, 060042, Bucharest, Romania,
bogoi_alina@yahoo.com, sterian.danaila@upb.ro*, ddisvoranu@gmail.com

DOI: 10.13111/2066-8201.2019.11.2.5

Received:26 April 2019/ Accepted: 06 May 2019/ Published: June 2019

7th International Workshop on Numerical Modelling in Aerospace Sciences "NMAS 2019"
15-16 May 2019, Bucharest, Romania, (held at INCAS, B-dul Iuliu Maniu 220, sector 6)
Section 2 – Flight dynamics simulation

Abstract: *The paper is a continuation of the efficiency and accuracy analysis of different high order numerical schemes previously published by the authors [1-3]. After the analysis of advection equation and the scalar conservation equation for different initial conditions and for different convex and non-convex conservative fluxes, we further investigated the one-dimensional conservation equation. This paper focuses on a new comparison of the behavior of the most known Weighted Essentially Non-Oscillatory (WENO) type numerical schemes for shock tube problem. We consider nine different Riemann Problems. Analytical solutions are provided for almost all different initial Riemann conditions. A third-order TVD Runge–Kutta (TVDRK3) scheme was adopted for advancing the solution in time. The motivation of this assessment is related to filling a gap in the specialized literature characterized by the bias towards presenting only cases favorable to a certain method. Our purpose is to present objectively the capacity of each method for solving one-dimensional conservation law problem. Unfortunately, not all the schemes identify accurately the position of the shocks or rarefaction waves and some of them even do not converge to a solution for different Riemann initial conditions.*

Key Words: *Conservative law, Riemann Shock tube problem, WENO-type schemes, Runge-Kutta schemes*

1. INTRODUCTION

Many fluid dynamics applications ranging from turbulent flows to acoustics include propagation of nonlinear waves with continuous or discontinuous distribution of the physical variables. Rarefaction fans, shocks or contact discontinuities are elementary waves that build-up the solution of Riemann problem for hyperbolic equations (e.g. Euler equations [4-5]). The aim of the present work is a new comparison of the behavior of the 5th-order WENO-type numerical methods, namely classical WENO-JS [6-9], mapped WENO[10], compact reconstruction WENO[11] and WENO-Z [12-13]. Let us consider the initial value problem of the one-dimensional vector conservative equation $\forall t \geq 0,\ x \in \mathbf{R}$:

$$\frac{\partial \mathbf{U}}{\partial t} + \frac{\partial \mathbf{F}(\mathbf{U})}{\partial x} = \mathbf{0}, \quad \mathbf{U}(x,0) = \mathbf{U}_0(x), \tag{1}$$

where $\mathbf{U}(x,t)$ and $\mathbf{F}(\mathbf{U}(x,t))$ are the conservative variables and respectively the conservative flux vector defined by:

$$\mathbf{U} = (\rho, \rho u, \rho E)^t, \quad \mathbf{F} = \left(\rho u, \rho u^2 + p, u(\rho E + p)\right)^t \tag{2}$$

and $\mathbf{U}_0(x)$ is the initial condition. Density ρ, velocity u, pressure p are related to the total energy E by the calorically perfect ideal gas equation of state

$$p = (k-1)\rho\left(E - u^2/2\right) \tag{3}$$

where *k* is the constant ratio of specific heats and equal to 1.4.

The numerical solution is obtained by discretizing the equation in space and time. The outcome of discretizing the spatial derivative for each corresponding point $x_j = j\Delta x,\ j = \overline{0,N}$, is the following conservative finite difference scheme:

$$\frac{\mathrm{d}\mathbf{U}_j}{\mathrm{d}t} + \frac{\mathbf{F}^*_{j+1/2} - \mathbf{F}^*_{j-1/2}}{\Delta x} = 0. \tag{4}$$

Thus, we get a system of ordinary differential equations for $\mathbf{U}_j(t) = \mathbf{U}(x_j,t)$. The term $\mathbf{F}_{j+1/2}$ is the numerical flux at cell boundaries computed by a Riemann solver $\mathbf{F}^*_{j+1/2} = \mathbf{F}^{\text{Riemann}}(\mathbf{U}^L_{j+1/2}, \mathbf{U}^R_{j+1/2})$.

The solution of the conservative finite difference formulation of eq. (1) written in the semi-discrete form, eq. (2), consists of two steps: spatial discretization and time marching, respectively.

2. SPATIAL DISCRETIZATION AND TEMPORAL DISCRETIZATION

In the frame of spatial discretization, we are interested in two essential steps in solution procedure: reconstruction of the physical fields to find the values at the left-and right-sides of cell boundaries, and evaluation of the numerical fluxes at cell boundaries that are needed in the Finite Volume Method (FVM) formulation to update the cell-integrated values for next time step.

For the first step, four different reconstruction schemes were analyzed: the original Weighted Essentially Non-Oscillatory (WENO) scheme, Mapped WENO (WENO-M), Compact Reconstruction WENO (CRWENO) schemes proposed by Ghosh and Baeder [11] and WENO-Z scheme proposed by Borges and al. [12]. The main interest of this paper is limited to present comparisons of numerical tests. Interested readers are guided towards the cited articles for theoretical background.

The evaluation of the numerical fluxes at cell boundaries is needed for updating the cell-integrated values for next time step and for solving the exact Riemann problem at the cell's boundary in the FVM formulation.

In this paper, for the second step we use the following typical numerical fluxes: the Roe flux, the HLL (Harten–Lax-van Leer)flux [5], the Lax–Friedrichs flux [9], the HLLL (Harten–Lax-van Leer-Linde) flux [14] and the AUSM flux [15]. As shown before, the numerical solution of the scalar conservation law amounts to solve the system of ODEs (eq. 4). The time discretization will be implemented using a third-order TVD Runge–Kutta (TVDRK3) developed by Shu and Osher [10].

3. NUMERICAL TESTS

In this section, we present the numerical results of some typical benchmark shock-tube tests for 1D Euler equation with different Riemann initial condition. The target is to verify the schemes for resolving the shock wave, contact discontinuity and rarefaction wave in compressible gas flows.

The shock tube problem considers a long, thin, cylindrical tube containing a gas separated by a thin membrane.

The gas is assumed to be at rest on both sides of the membrane, but it has different constant pressures and densities on each side. At time $t = 0$, the membrane is broken, and the problem is to determine the ensuing motion of the gas which generates a nearly centered wave system that typically consists of a rarefaction/shock wave, a contact discontinuity and a shock/ rarefaction wave.

The middle wave is always a contact discontinuity while the left and right (non-linear) waves are either shock or rarefaction waves.

Therefore, according to the type of nonlinear waves there can be four possible wave patterns [5]. This physical problem is reasonably well approximated by solving the shock-tube problem for the Euler equations.

The solution to this problem (known as Riemann problem) consists of a shock wave moving into the low pressure region, a rarefaction wave that expands into the high pressure region, and a contact discontinuity which represents the interface.

For the most of the numerical tests, the computational domain is taken as $[0, 1]$ with zero gradient boundary conditions. Any different conditions will be specifically mentioned.

3.1 Sod's shock tube problem (expansion-contact-shock)

The initial condition for the Sod problem [5] is

$$(\rho, u, p) = \begin{cases} (1, 0, 1), & 0 \le x < 0.5 \\ (0.125, 0, 0.1), & 0.5 \le x \le 1 \end{cases} \tag{5}$$

and the final computation time is $t = 0.15$.

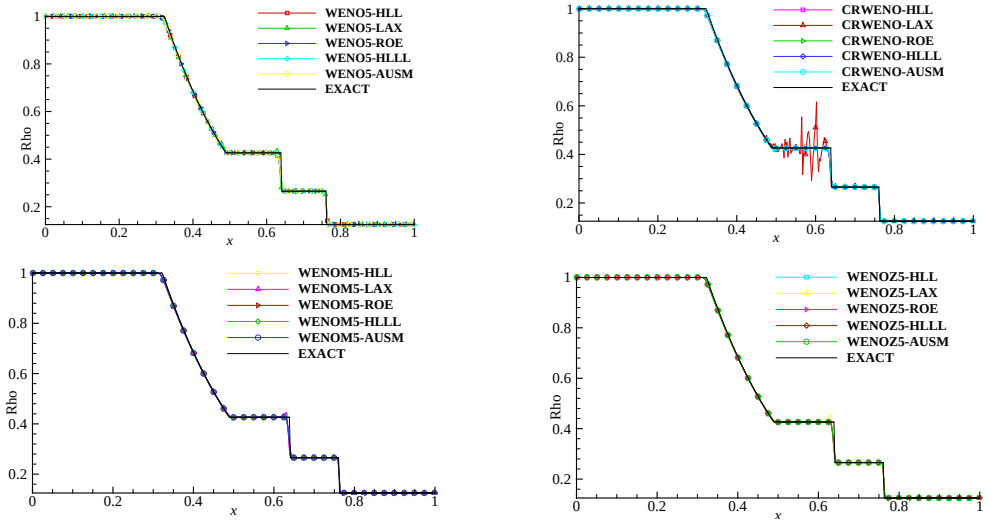

Fig. 1a Numerical results for the density for Sod's shock tube problem at t = 0.15

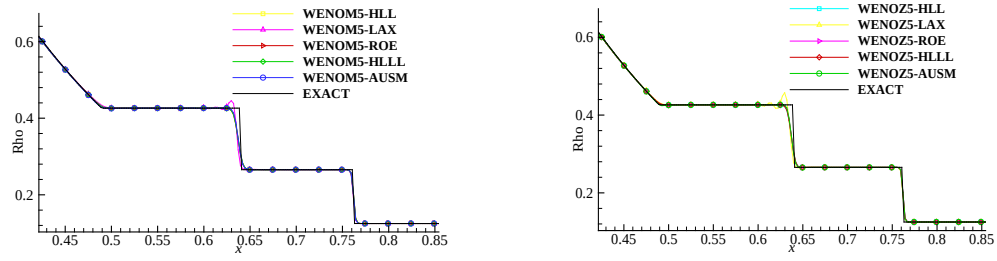

Fig. 1b Numerical results for the density for Sod's shock tube problem at t = 0.15(details)

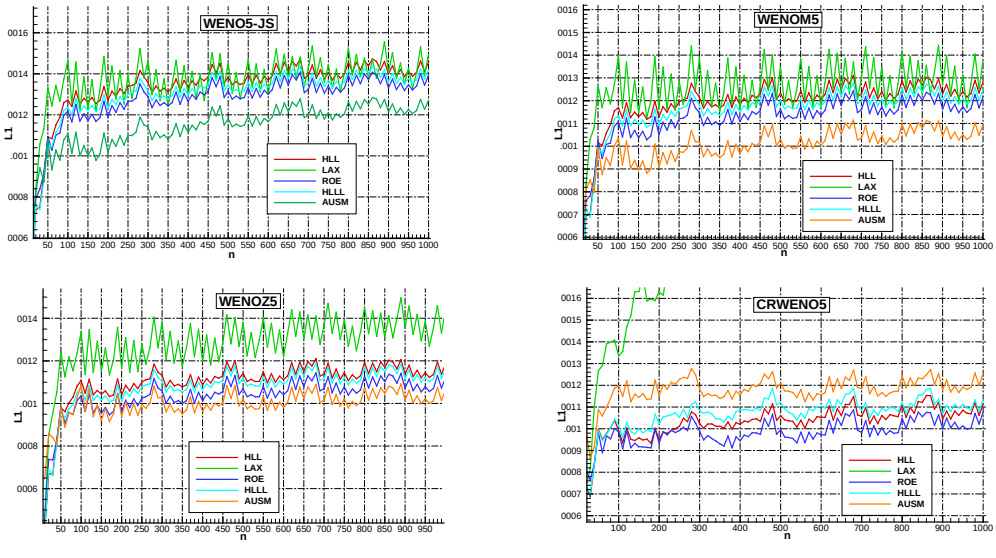

Fig. 1c L1-error of the density for Sod's shock tube problem up to t = 0.15

The grid resolution is 400 cells and the time stepping condition is CFL = 0.3. Figures 1a-b illustrate well the resolved shock and contact solutions.

Predictions given by the WENO-type schemes are indistinguishable at the given scale. Nevertheless, the numerical solution displays a gradual departure from the analytical solution in the regions with sharp slopes. Quantitative information regarding the global error is given in Fig. 1c in terms of the L1-error for the density. The minimal global error is obtained by the reconstruction with classical WENO5, WENOM and WENOZ in combination with the AUSM flux and shows that the error is around 0.001. CRWENO gives better results in combination with ROE flux. The combination CRWENO-Lax flux exhibit slight oscillations in the vicinity of the contact wave, hence poor results.

3.2 Lax's shock tube problem (expansion-contact-shock)

The initial condition for the Lax problem [5] is

$$(\rho, u, p) = \begin{cases} (0.445, 0.698, 3.528), & 0 \le x < 0.5 \\ (0.5, 0, 0.571), & 0.5 \le x \le 1 \end{cases} \tag{6}$$

and the final time is $t = 0.12$. Figures 2a-b show no spurious oscillations at any shock or contact discontinuity and the evolutions given by all WENO-type schemes are similar at the represented scale.

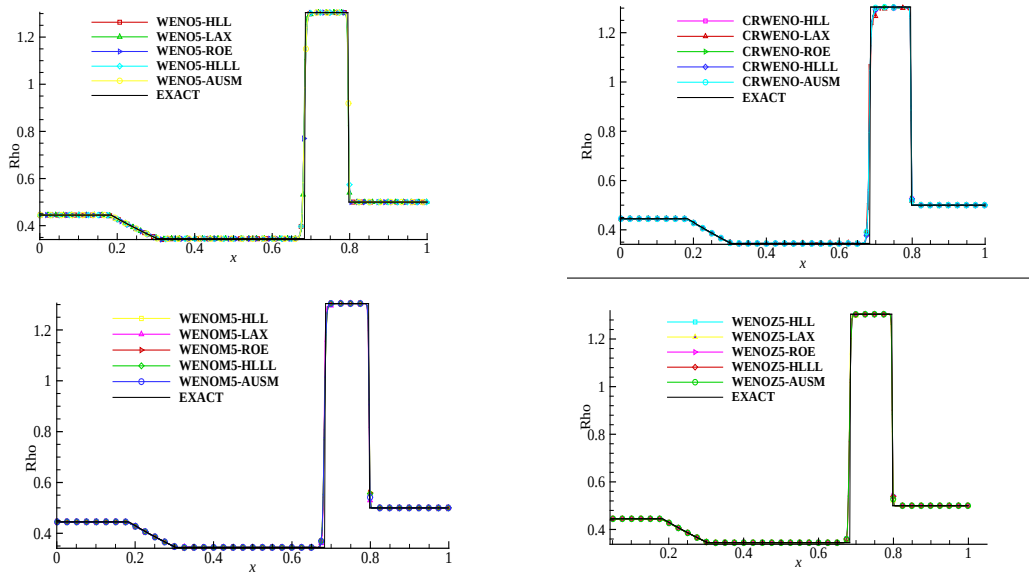

Fig. 2a Numerical results of the Lax's shock tube problem for density at t = 0.12

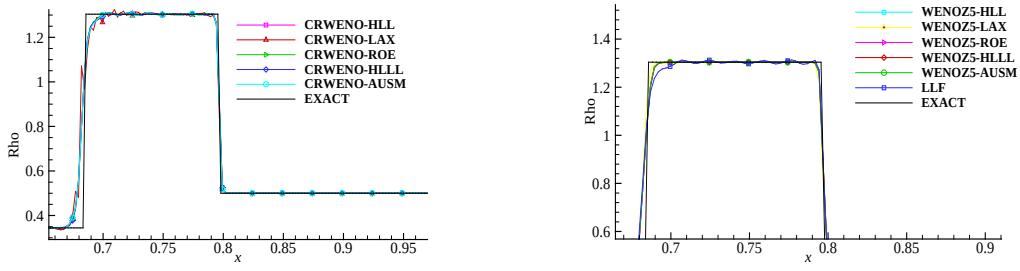

Fig. 2b Numerical results of the Lax's shock tube problem for density at t = 0.12 (details)

Nevertheless, the numerical solution displays a gradual departure from the analytical solution in the regions with sharp slopes. Quantitative information regarding the global error is given in Fig. 2c which presents the L1-error for the density.

The minimal global error is obtained by the reconstruction with classical WENO5, WENOM and WENOZ in combination with the flux AUSM, exhibiting an error around 0.001.

An unexpected good accuracy (i.e. around 0.035) is obtained by the combination between the reconstruction with classical WENO5, WENOM and WENOZ and the Lax flux. The fluxes HLL and HLLL give identically numerical results for almost all reconstructions methods, excepting CRWENO.

CRWENO gives better results in combination with ROE flux. The combination CRWENO-Lax flux gives high oscillations in the vicinity of the contact wave and therefore, not acceptable results.

An unexpected good accuracy (i.e. around 0.035) is obtained by the combination between the reconstruction with classical WENO5, WENOM and WENOZ and the Lax flux.

The fluxes HLL and HLLL give identically numerical results for almost all reconstructions methods excepting CRWENO. CRWENO gives better results in combination with ROE flux.

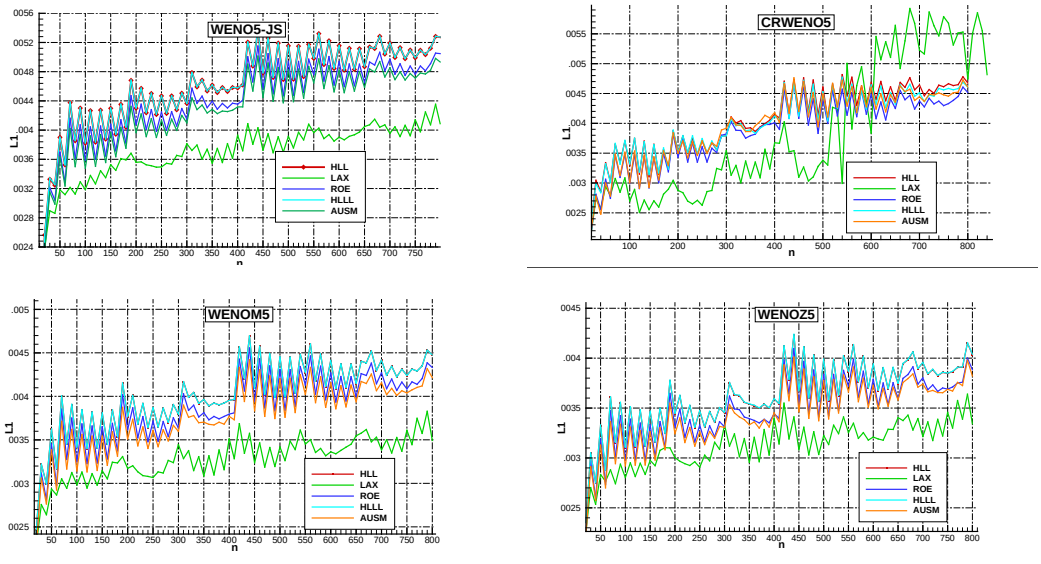

Fig. 2c L1-error of the density for the Lax's shock tube problem up tot = 0.12

3.3 Strong shock tube problem (expansion-contact-shock)

The initial condition for the strong shock tube problem[16] is

$$(\rho,\, u,\, p) = \begin{cases} (1, 0, 10^{10}), & 0 \le x < 0.5 \\ (0.125, 0, 0.1), & 0.5 \le x \le 1 \end{cases} \tag{7}$$

and the final time is $t = 2.5 \cdot 10^{-6}$. This initial condition creates a supersonic shock associated with extreme jumps in velocity and pressure, see Fig. 3a. It is well known that purely non-conservative schemes fail to compute strong shocks due to their intrinsic inability to calculate correct shock speeds. The combination CRWENO-Lax flux gives high oscillations in the vicinity of the contact wave and therefore, not acceptable results.

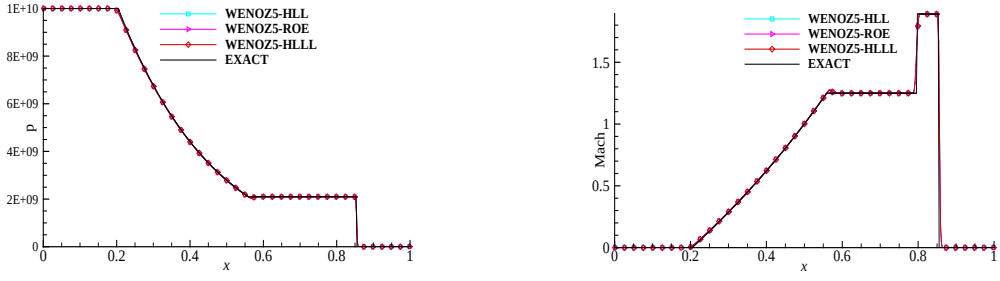

Fig. 3a Pressure and Mach number for the strong shock tube problem at t = 2.5 10^{-6}

Fig. 3b shows there are density overshoots in results but correct shock calculation. We have also remarked that AUSM scheme does not converge in most of the cases. The only case where it worked (n.b., but not very accurate), is with the CRWENO method. Instead, Lax flux gives high oscillations in the vicinity of the contact wave. Figure 3c shows selected relevant details from Fig. 3b. Quantitative information regarding the global error is given in Fig. 3d, in terms of the L1-error for the density.

The minimal global error is delivered by the reconstruction with WENOZ method and is less than 0.0035 for all combinations of fluxes.

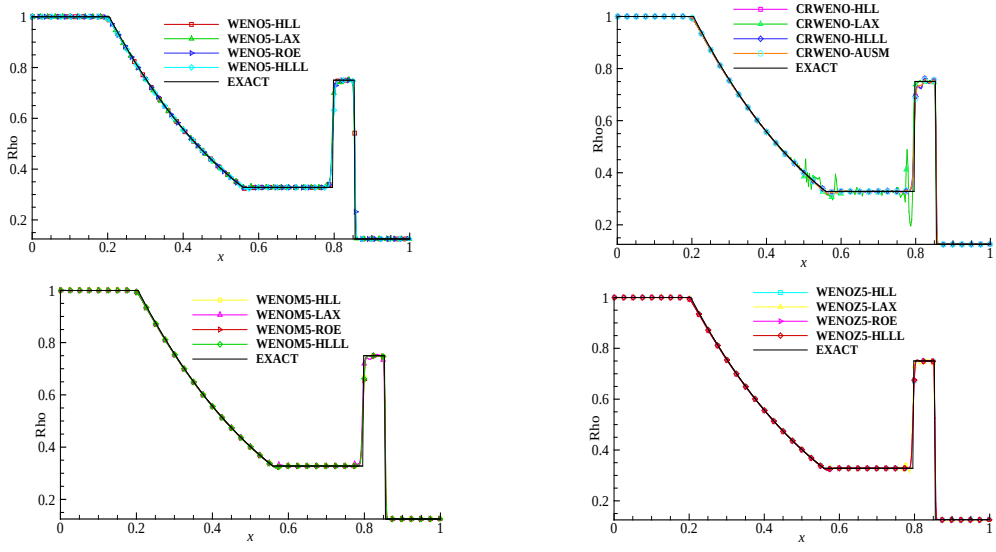

Fig. 3b Numerical results of the strong shock tube problem for density at t = 2.5 · 10^{-6}

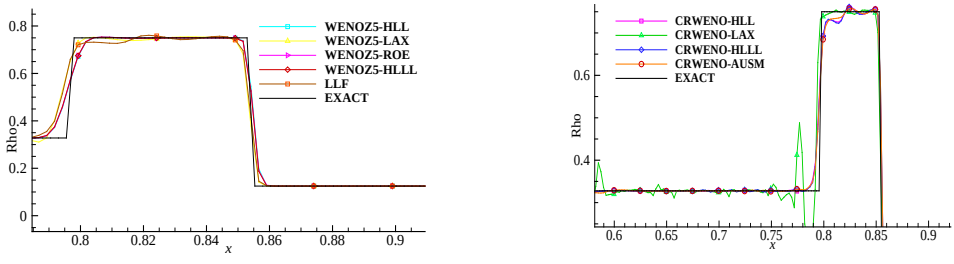

Fig. 3c Numerical results of the strong shock tube problem for density at t = 2.5 · 10^{-6}(details)

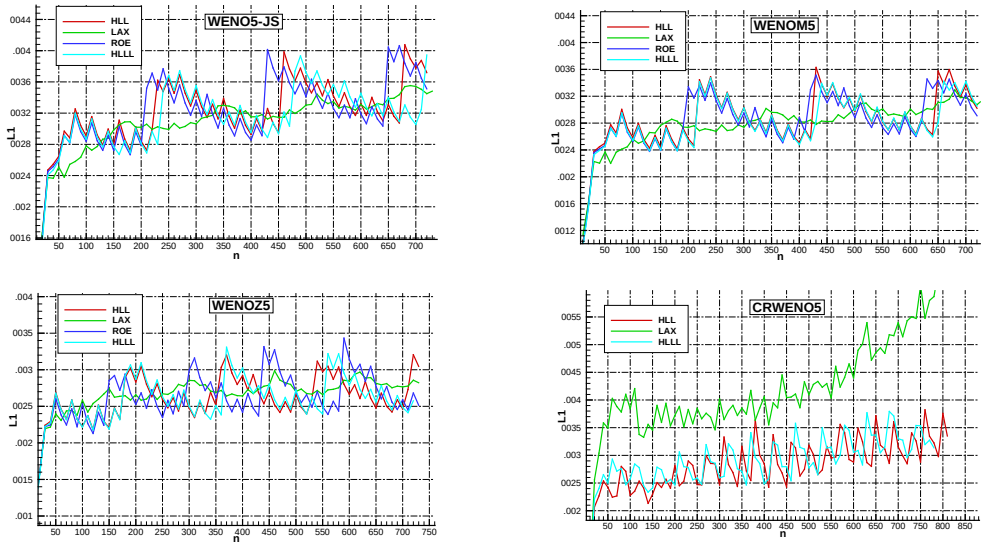

Fig. 3d L1-errorof the density for the strong shock tube problem up to t = 2.5 10^{-6}

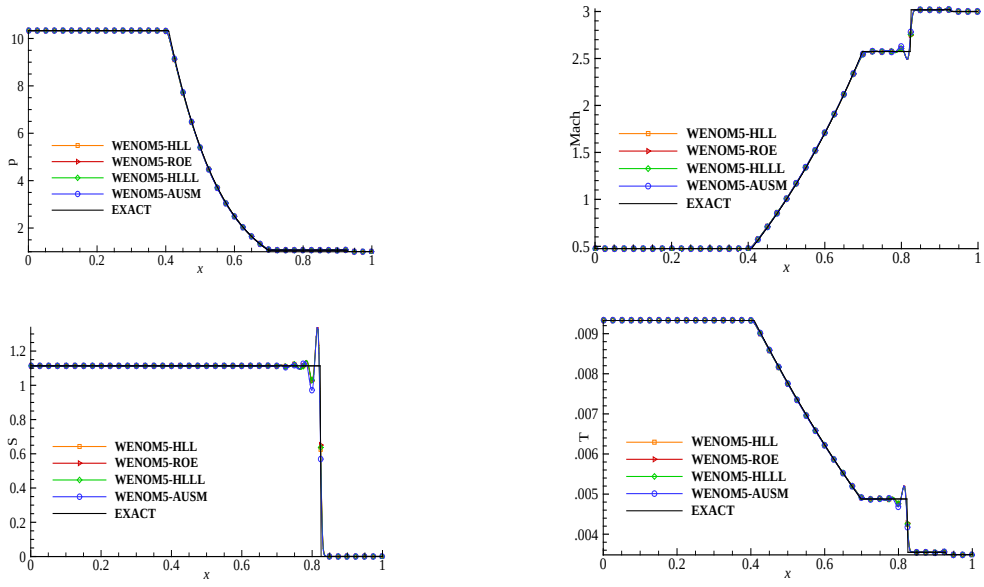

Fig. 4a Pressure, Mach number, entropy and temperature evolution for of the Mach 3 shock tube problem at t = 0.09

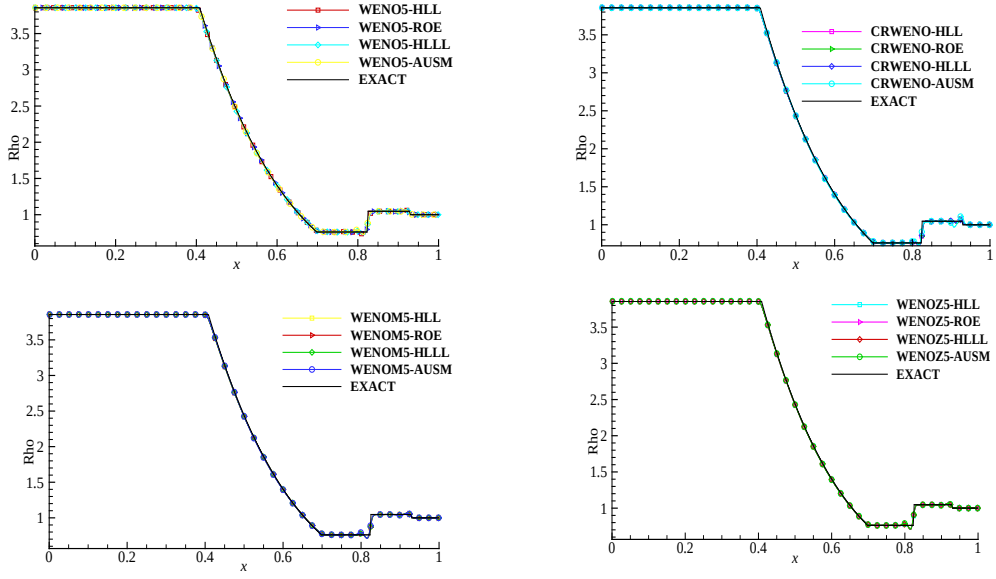

Fig. 4b Numerical results for density of the Mach 3 shock tube at t = 0.09

3.4 Mach 3 shock test (expansion-contact-shock)

The Mach 3 shock tube experiment [17] uses the following initial conditions,

$$(\rho,\, u,\, p) = \begin{cases} (3.857, 0.92, 10.3333), & 0 \le x < 0.5 \\ (1, 3.55, 1), & 0.5 \le x \le 1 \end{cases} \tag{8}$$

and the final time is $t = 0.09$. Figure 4a shows no evident spurious oscillations at any shock or contact discontinuities. Although not represented, the only exception of poor behavior is

the combination with Lax flux. In all cases we notice a small wavelet at shock discontinuity, see Fig. 4b and Fig. 4c. The L1-error given in Fig. 4d revealed once again that WENOZ method with all fluxes combinations gives the best accuracy. We chose to ignore the error of Lax-Friedrichs flux as it yielded huge errors. We also remarked that using HLLL flux in almost all reconstructions gave smaller errors in comparison with other fluxes.

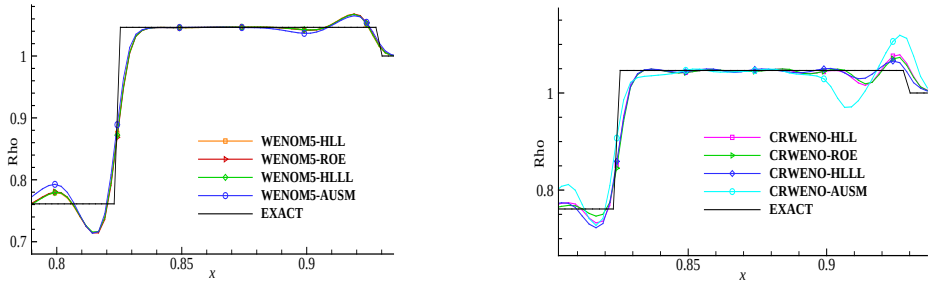

Fig. 4c Numerical results of for density the Mach 3 shock tube at t = 0.09 (details).

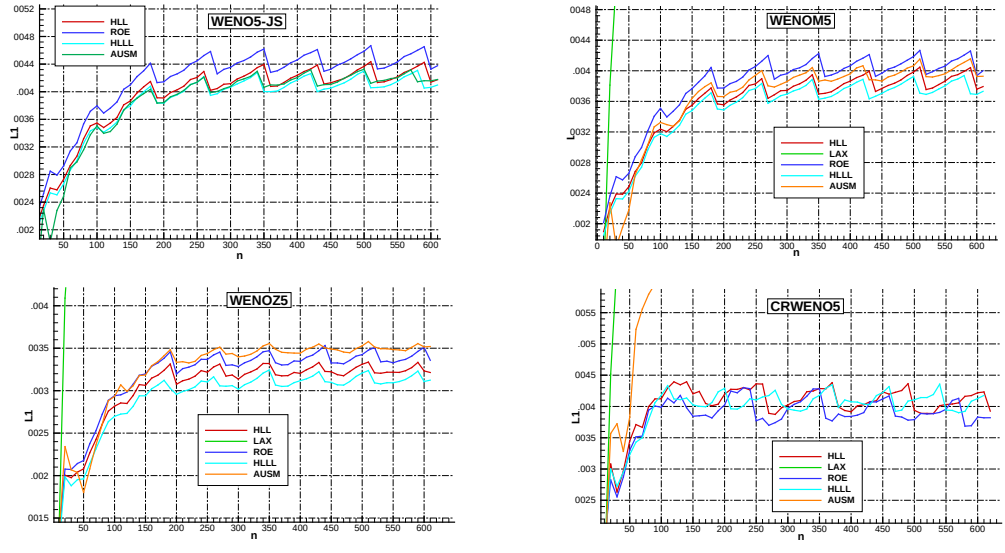

Fig. 4d L1-error of the density for the Mach 3 shock tube up to t = 0.09

3.5 High Mach flow test (shock-contact-shock)

The high Mach flow test experiment [18] uses the following initial conditions,

$$(\rho, u, p) = \begin{cases} (10, 2000, 500), & 0 \le x < 0.5 \\ (20, 0, 500), & 0.5 \le x \le 1 \end{cases} \tag{9}$$

and the final time is $t = 0.09$.

Numerical solution using WENO-M method is given in Fig. 5a. An unexpected result was discovered regarding CRWENO and WENO-Z method. Figure 5b shows that only WENO-JS and WENO-M produced acceptable numerical solutions to this problem.

CRWENO in combination with any flux was divergent and therefore it was not displayed.

WENO-Z does not converge with any flux, except when using the Lax flux. However, in this case the accuracy was poor.

Figure 5c presents in detail the evolution of density for WENO-JS and WENO-M method which looks very similar in both cases.

Nevertheless, the evolutions of L1-error with respect to density presented in Fig. 5d show that WENO-M combination yielded better results than WENO-JS. We notice that in this case, at high Mach numbers, AUSM behaves much better than in the previous cases. The results are similar to those produced by HLL or Roe fluxes.

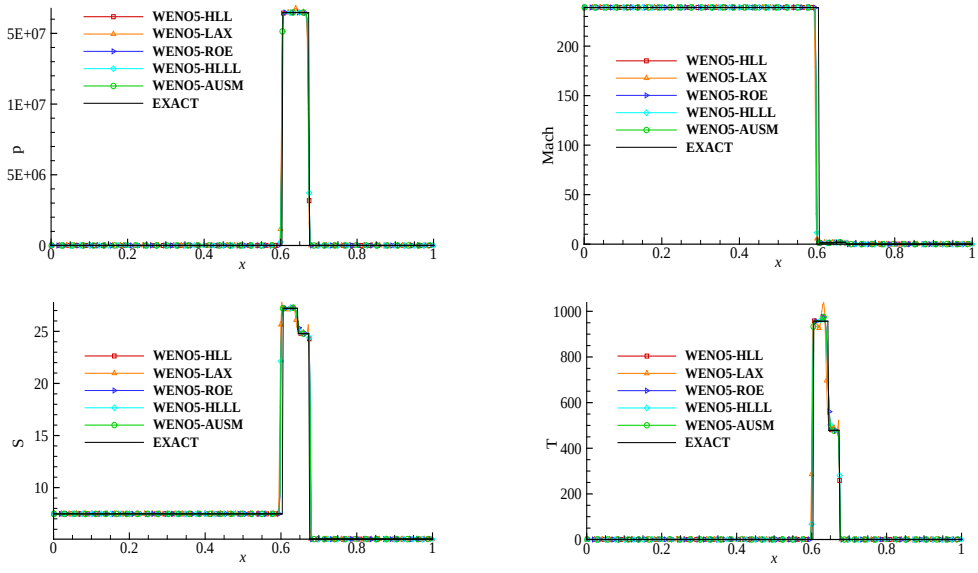

Fig. 5a Pressure, Mach number, entropy and temperature evolution for high Mach number shock tube problem at t = 1.75 10^{-4}

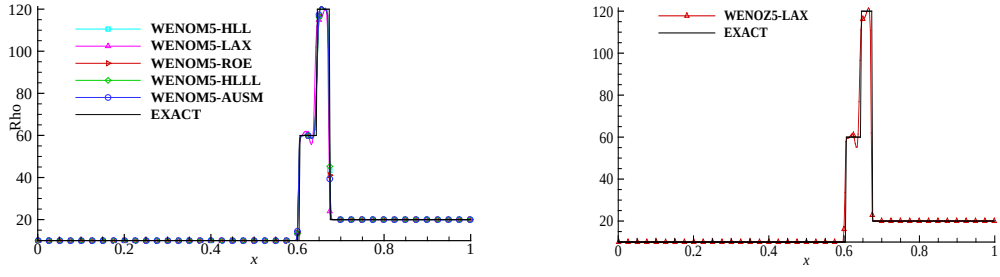

Fig. 5b Numerical results of the high Mach number shock tube problem at t = 1.75 · 10^{-4}

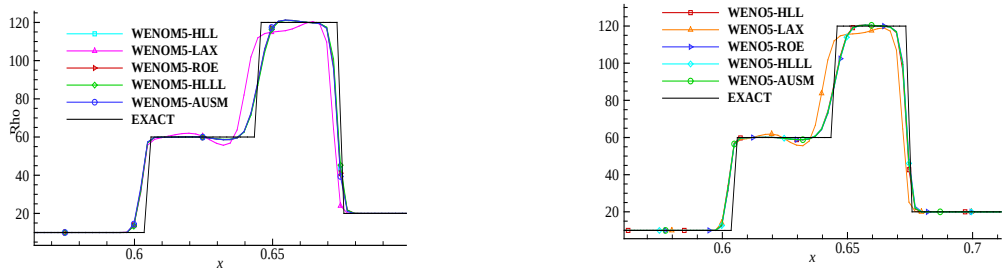

Fig. 5c Numerical results of the high Mach number shock tube problem at t = 1.75 10^{-4}(details)

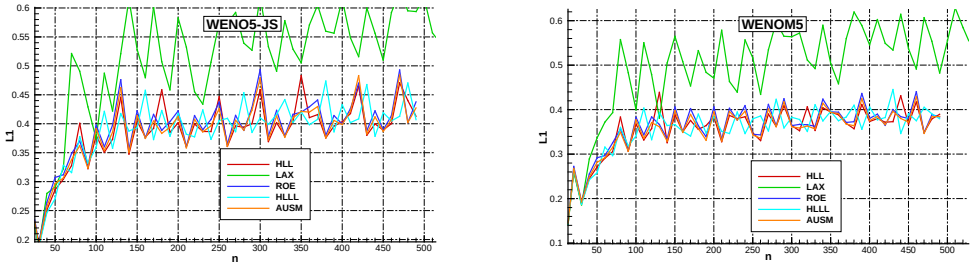

Fig. 5d L1-error of the density for the high Mach number shock tube problem up to t = 1.75 10^{-4}

3.6 Two symmetric rarefaction waves (expansion-contact-expansion)

The two symmetric rarefaction waves experiment [5] uses the following initial conditions

$$(\rho, u, p) = \begin{cases} (1, -2, 0.4), & 0 \le x < 0.5 \\ (1, 2, 0.4), & 0.5 \le x \le 1 \end{cases} \tag{10}$$

and the final time is $t = 0.15$.

Fig. 6a reveals the unexpected fact that only two reconstruction methods: WENO-JS and WENO-M in combination with Roe flux are capable to provide a solution for this problem.

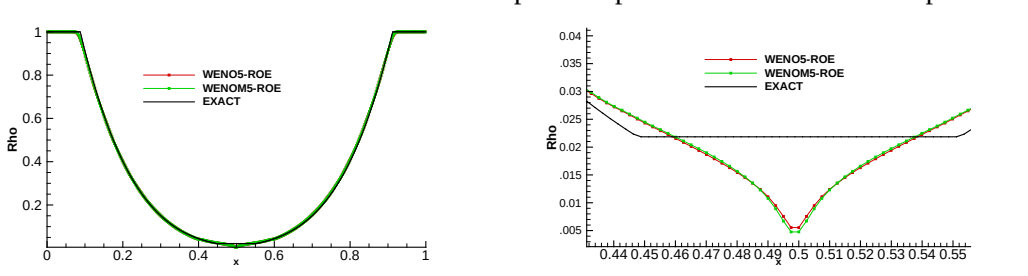

Fig. 6a Numerical results of the two symmetric rarefaction waves problem computed at t = 0.15 (details)

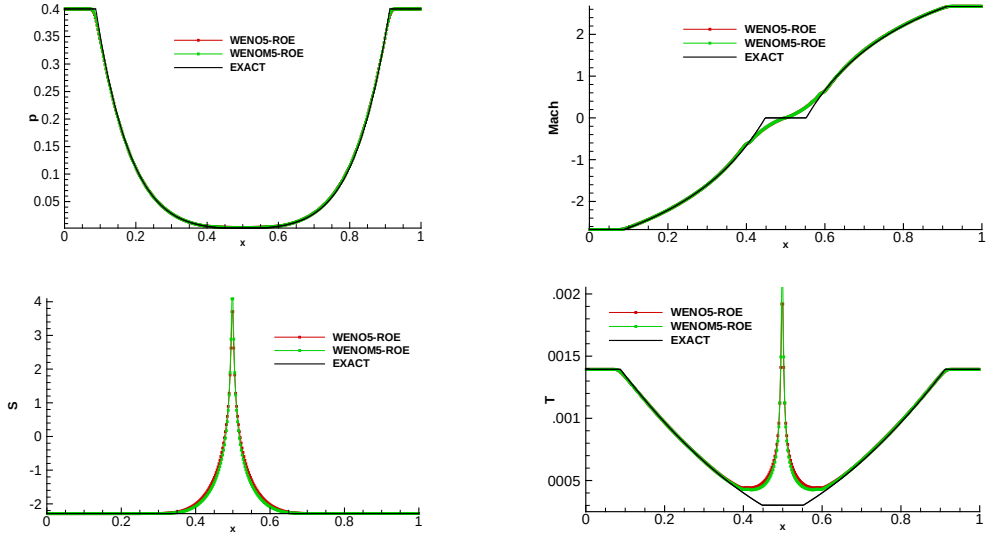

Fig. 6b Pressure, Mach number, entropy and temperature evolution for the two symmetric rarefaction waves problem at t = 0.15

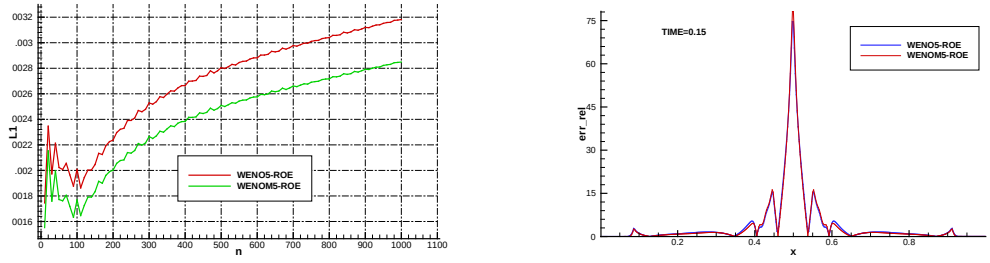

Fig. 6c L1-error of the density for the two symmetric rarefaction waves up to t = 0.15 (left). Relative error at t = 0.15

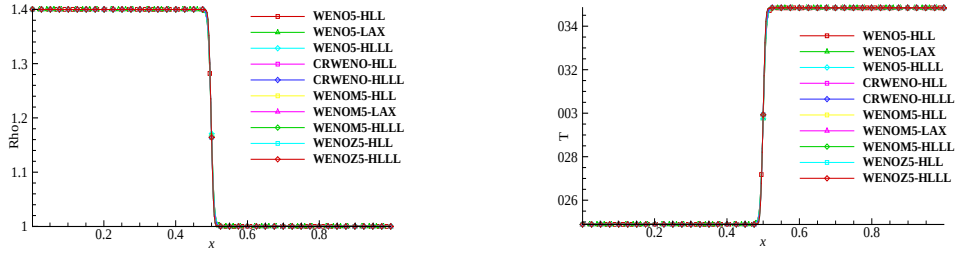

Fig. 7. The density profile of the stationary contact discontinuity at t =2

The distribution profiles for all variables (density, pressure, temperature, entropy) are accurately obtained in the whole domain except in the vicinity of $x = 0.5$, where the results are completely erroneous. This result is confirmed in Fig. 6b for the rest of variables. Entropy must be constant everywhere but the results are wrong. In the neighborhood of 0.5 (Fig. 6c), the relative error increases up to 75% for both reconstruction methods. L1-error suggests that WENOM5 gives better results than WENO5 for all time range of the simulation.

3.7 Stationary contact discontinuity

A stationary contact discontinuity [16] is initially established by setting the following conditions,

$$(\rho, u, p) = \begin{cases} (1, -2, 0.4), & 0 \le x < 0.5 \\ (1, 2, 0.4), & 0.5 \le x \le 1 \end{cases} \tag{11}$$

and the final time is $t = 2$. No motion at all is expected and the solution should remain frozen at its initial state. As shown in Fig. 7, the initial jump in density remains at its initial condition. Other physical quantities (not shown here) remain constant. Figure 7 demonstrates that all schemes converge to the exact solution.

3.8 Interaction of blast waves

This problem, introduced by Woodward and Colella [18], involves multiple interactions of strong shock waves and other discontinuities. Initial conditions are,

$$(\rho, u, p) = \begin{cases} (1, 0, 10^{3}), & 0 \le x < 0.1 \\ (1, 0, 10^{-2}), & 0.1 \le x < 0.9 \\ (1, 0, 10^{2}), & 0.9 \le x \le 1 \end{cases} \tag{12}$$

and the final time is $t = 0.038$.

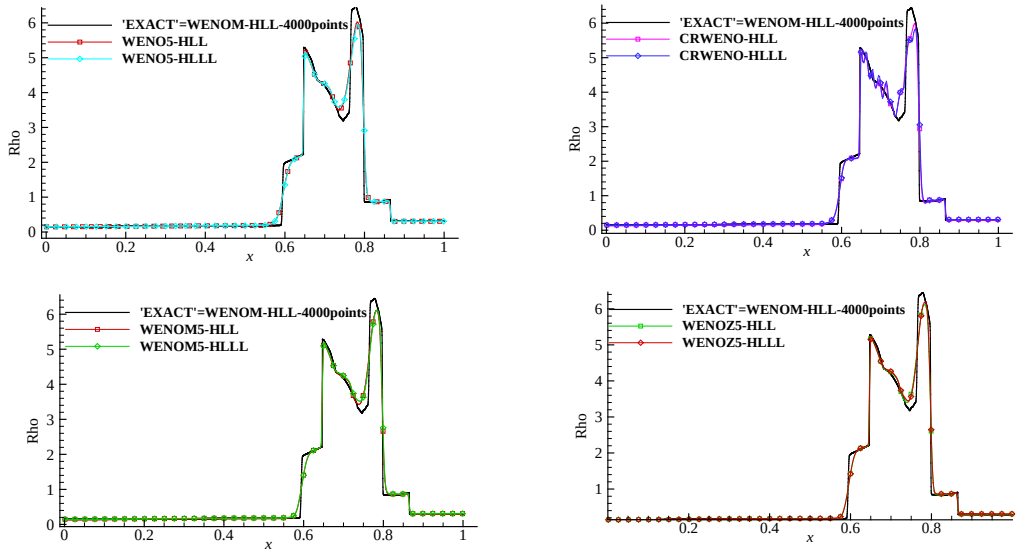

Fig. 8a Solution for density of the interactive blast waves problem at t=0.038

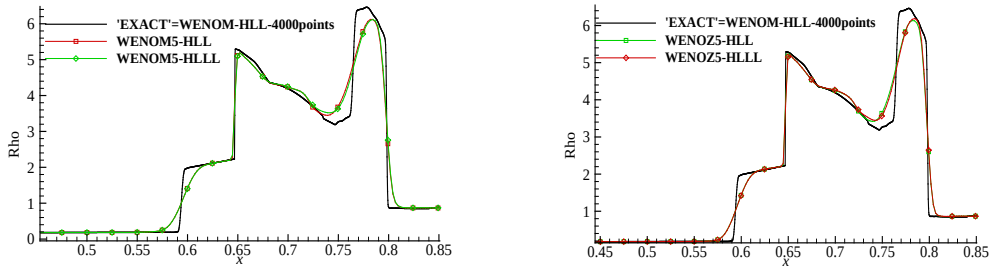

Fig. 8b Solution for density of the interactive blast waves problem at t=0.038(details)

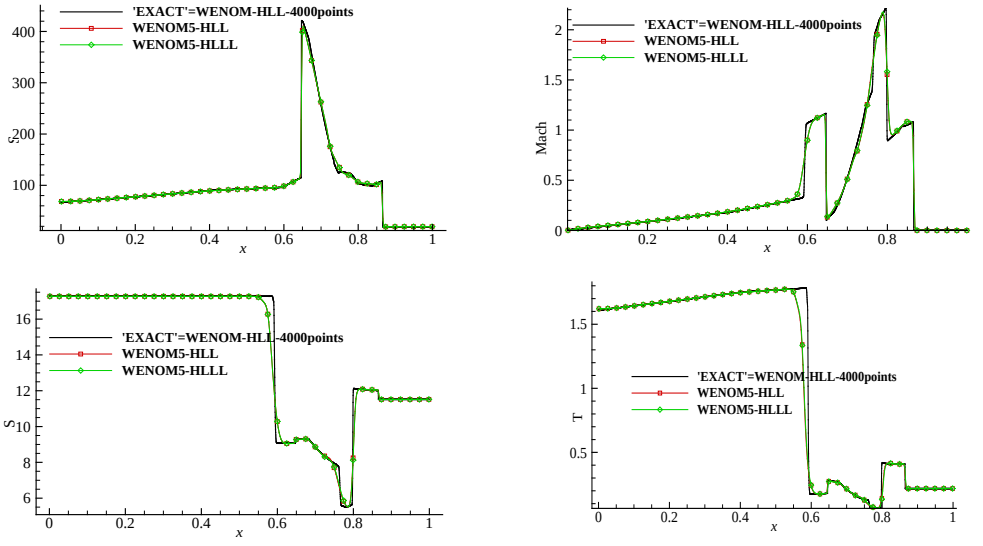

Fig. 8c Pressure, Mach number, entropy and temperature evolution for interactive blast waves problem at t=0.038

We considered reflective solid wall conditions for the boundary at $x=0$ and at $x=1$. Figure 8a and figure 8b demonstrate that all four schemes converge to the reference solution (n.b. 'Exact') computed by the WENO-M-HLL combination with $N = 4000$ points.

Once again we can remark that flux AUSM and Roe are not capable to solve this problem. As before, WENO-M and WENO-Z show an improved convergence with respect to WENO-JS and CRWENO, due to their smaller dissipation for the same fluxes. In Fig. 8c entropy and Mach number are better predicted than entropy and temperature for both fluxes HLL and HLLL.

3.9 SHU-OSHER test

This case is proposed by Shu and Osher [19]. A one-dimensional Mach 3 shock wave interacts with a perturbed density field generating both small scale structures and discontinuities.

Hence it is selected to validate shock-capturing and wave-resolution capability. The initial condition is given in the domain $[-5,\ 5]$ as

$$(\rho,\ u,\ p)=\begin{cases}(27/7,\ 4\sqrt{35}/9,\ 31/3), & -5\le x<-4\\ (1+0.2\sin 5x,\ 0,\ 1), & -4\le x\le 5\end{cases} \tag{13}$$

and the final time is $t=2$.

The reference "exact" in the legends of Figs. 9 refers to a solution obtained by the fifth-order WENO-schemes with $N = 4000$.

Figure 9a and 9b show that all schemes combined with all fluxes are capable of successfully capturing the acoustic waves with shocklets.

However, any WENO combination with AUSM flux gives poor accuracy even for N=4000 points (see Fig. 9c).

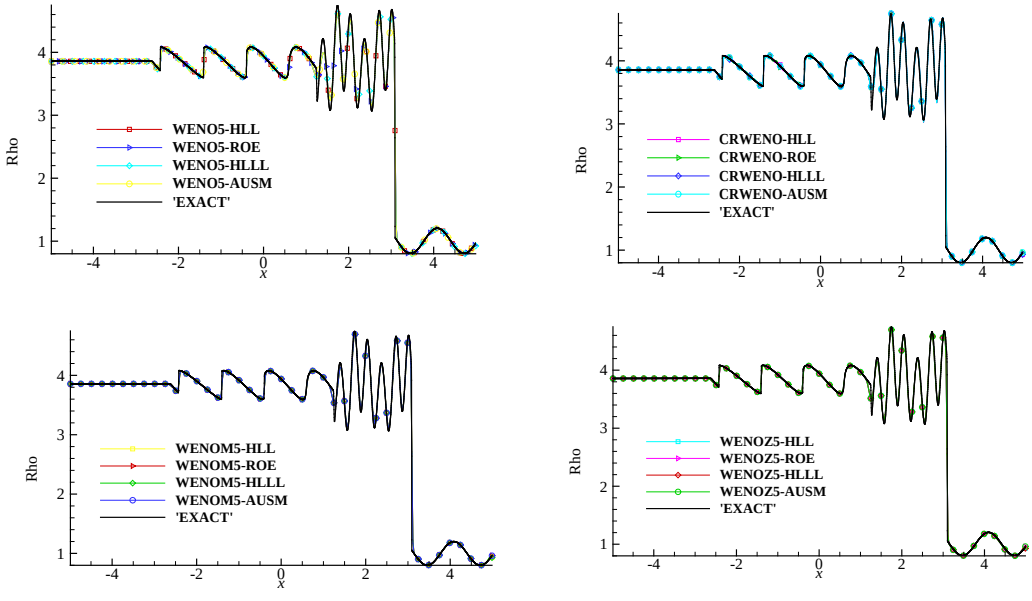

Fig. 9a Solution for density of the Shu-Osher shock–density wave interaction at *t*=2

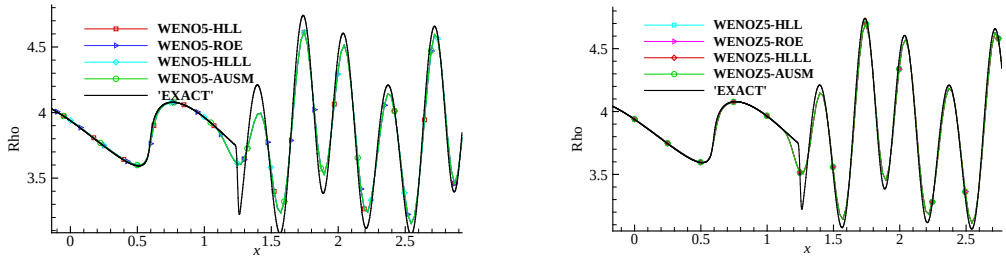

Fig. 9b Solution for density of the Shu-Osher shock–density wave interaction at t=2 (details)

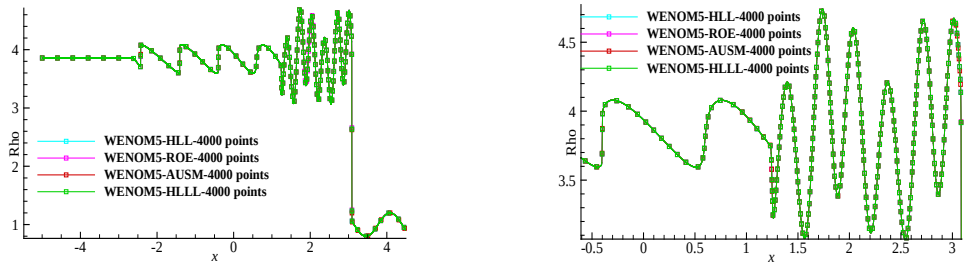

Fig. 9c Solution for density of the Shu-Osher shock–density wave interaction at t=2 for N=4000

4. CONCLUSIONS

The purpose of this article is to give a general perspective and to present objectively the capacity of each WENO method to solve the shock tube problem with different initial conditions. These benchmark tests are relevant in order to check and identify accurately the position of the shock, contact and rarefaction waves in each situation.

For the first two classical shock tube problems, the predictions are indistinguishable at the illustrated scale. However, looking more closely, the quantitative information regarding the global shows that not all combinations of reconstruction methods and fluxes produce accurate solutions in time. Thus, for *Sod's problem* the flux AUSM with WENO5, WENOM and WENOZ gave best results while for the *Lax's problem*, the combinations of Lax-flux with WENO5, WENOM and WENOZ were the most accurate. CRWENO-Roe gives good numerical results. For the *Strong shock tube problem* the AUSM scheme does not converge in most cases. The only case where it works (n.b. but not very accurate) is with CRWENO method. Instead, Lax flux yielded high oscillations in the vicinity of the contact wave. The minimal global error is provided by the reconstruction with WENOZ method exhibiting an error less than 0.0035 for all combinations of fluxes. For the *Mach 3 shock test* we notice in all cases a small wavelet at shock discontinuity. The L1-error revealed once again that WENOZ method with all fluxes combinations gives the best accuracy. We chose to ignore the error of Lax-Friedrichs flux as it was huge. We also remarked that flux HLLL in almost all reconstructions cases gives smaller errors in comparison with other fluxes. Continuing with the *High Mach flow test* we discovered that CRWENO and WENO-Z method did not converge at all and only WENO-JS-AUSM and WENOM-AUSM gave reasonable numerical solutions to this problem. The *Two symmetric rarefaction waves test* reveals that only two reconstruction methods: WENO-JS and WENOM in combination with Roe flux are capable of reaching a solution for this problem. All the variables like density, pressure, temperature, entropy are accurately obtained everywhere, except in the vicinity of $x = 0.5$ where the

results are completed erroneous. L1-errors suggest that WENOM gives better results. The *Stationary contact discontinuity case* demonstrates that all schemes converge to the exact solution. For the *Interaction of blast waves test* and for *SHU-OSHER test* the reference solution (n.b. 'Exact') is computed by the WENOM-HLL combination with $N = 4000$ points. Once again we can remark that AUSM and Roe fluxes are not capable of solving this problem. As before, WENOM and WENOZ showed an improved convergence with respect to WENO-JS and CRWENO, due to their smaller dissipation for the same fluxes. Finally, we can conclude that the combination WENOZ-AUSM works very well for reasonable discontinuities in pressure, velocity and density and extreme jumps in velocity and pressure. WENOZ works similarly for all fluxes, except for the Lax and AUSM.

REFERENCES

[1] A. Bogoi, D. Isvoranu, S. Dănăilă, Assessment of some high-order finite difference schemes on the scalar conservation law with periodical conditions, *INCAS BULLETIN*, vol. **8**, pp.77 – 92, 2016.

[2] S. Dănăilă, A. Bogoi, D. Isvoranu, Some Mandatory Benchmark Tests for Stability and Accuracy of High-Order Finite Difference Schemes, *Applied Mechanics and Materials*, **859**, pp. 52-56, 2017.

[3] A. Bogoi, S. Dănăilă, D. Isvoranu, Assessment of three WENO type schemes for nonlinear conservative flux functions, *INCAS BULLETIN*, **10**, pp.77 – 92, 2018.

[4] S. Dănăilă, C. Berbente, *Metode numerice în dinamica fluidelor (Numerical Methods in Fluid Dynamics)*, Ed. Academiei, 2003.

[5] E. F. Toro, *Riemann Solvers and Numerical Methods for Fluid Dynamics: A Practical Introduction*, third edition, Springer-Verlag, 2009.

[6] F. Aràndiga, A. Baeza, A. M. Belda, and P. Mulet. Analysis of WENO schemes for full and global accuracy. *SIAM J. Numer. Anal.*, **49**, pp. 893–915, 2011.

[7] A. Harten, B. Engquist, S. Osher, S.R. Chakravarthy, Uniformly high order accurate essentially non-oscillatory schemes, III, *J. Comput. Phys*., vol. **71**, pp. 231–303, 1987.

[8] X.-D. Liu, S. Osher, and T. Chan, Weighted essentially non-oscillatory schemes, *J. Comput. Phys*., **115**, pp. 200–212, 1994.

[9] C. W. Shu, Essentially non-oscillatory and weighted essentially non-oscillatory schemes for hyperbolic conservation laws, *NASA/CR-97-206253 ICASE Report*, pp. 97- 65, 1997.

[10] A. K. Henrick, T. D. Aslam, J. M. Powers, Mapped weighted essentially non-oscillatory schemes: achieving optimal order near critical points, *J. Comput. Phys*., **207**, pp. 542–567, 2005.

[11] D. Ghosh, J. D. Baeder, Compact Reconstruction Schemes with Weighted ENO Limiting for Hyperbolic Conservation Laws, *SIAM Journal on Scientific Computing*, **34**, pp. 1678–1706, 2012.

[12] R. Borges, M. Carmona, B. Costa, W. S. Don, An improved weighted essentially non-oscillatory scheme for hyperbolic conservation laws, *J. Comput. Phys*. **227**,pp. 3191–3211, 2008.

[13] F. Acker, R. d. R. Borges, B. Costa, An improved WENO-Z scheme, *J. Comput. Phys*., 313 (2016) 726–753.

[14] T. Linde, A Practical, General-Purpose, Two-State HLL Riemann Solver for Hyperbolic Conservation Laws, *International Journal for Numerical Methods Fluids*, **40**, pp. 391-402, 2002.

[15] M.-S. Liou and C. J. Steffen, A New Flux Splitting Scheme, *J. Comput. Phys*, **107**, pp. 23-39, 1993.

[16] F. Xiao, R. Akoh, S. Ii, Unified formulation for compressible and incompressible flows by using multi integrated moments II: multi-dimensional version for compressible and incompressible flows, *J. Comput. Phys*., **213**, pp. 31-56, 2006

[17] S. Y. Kadioglu, M. Sussman, S. Osher, J. P. Wright, and M. Kang, A Second Order Primitive Preconditioner For Solving All Speed Multi-Phase Flows, *J. Comput. Phys*.**209**, pp. 477-503, 2005.

[18] P. Woodward, P. Colella, The numerical simulation of two-dimensional fluid flow with strong shocks, *J. Comput. Phys.*, **54**, pp. 115, 2008.

[19] C. W. Shu, S. Osher, Efficient implementation of essentially nonoscillatory shock-capturing schemes, ii, *J. Comput. Phys.*, **83** , pp.32–78, 2008.